

# TMT - Stressed Mirror Polishing Fixture Study

Stephen F. Sporer  
Tinsley Laboratories, Division of SSG Precision Optronics,  
4040 Lakeside Drive, Richmond, CA 94806, USA

## ABSTRACT

This paper examines the use of Stressed Mirror Polishing for rapid and low cost fabrication of the large number of mirror segments required for the TMT primary mirror. Prior experience fabricating Keck mirror segments is used as a starting point. Specific refinements are made to processes and tooling for faster and more economical fabrication of segments ready for Ion Beam Figuring. Analytical calculations, finite element analyses, design trades, and stressing fixture conceptual designs are presented. Feasibility of Stressed Mirror Polishing is demonstrated and recommendations for further work are given.

Keywords: TMT, Thirty Meter Telescope, SMP, Stressed Mirror Polishing, primary mirror, segment fabrication, large optics

## 1. INTRODUCTION

Stressed Mirror Polishing (SMP) is the technique of applying specific loads to a part to warp out the non-spherical components of surface shape, then grinding and polishing the part spherical. After polishing, the warping loads are removed and the part springs back to a stress-free state with the desired aspheric surface shape. Spherical processing is much faster than alternative aspheric (small tool) processes because much larger tools are used and the entire surface is worked at once. The purpose of this paper is to demonstrate the feasibility of SMP for rapidly producing the large number of mirror segments required for the TMT primary mirror.

## 2. BACKGROUND

The TMT primary mirror design is a nearly parabolic conic of revolution with a 60 meter paraxial Radius Of Curvature (ROC) and a 30 meter diameter. There are 123 unique mirror segments (each a slightly irregular hexagon) with 6-fold rotational symmetry (plus one set of spares) requiring a total of 861 segments.

The exact distribution of local segment origins and hex corner coordinates has not yet been determined by the TMT program office and is beyond the scope of this paper<sup>3</sup>. For this report we assume segment origins laid out on a regular hexagonal grid when viewed down the parent axis, and regular hexagonal segments measuring 1.20 m across the corners.

The sag of each segment is approximately 3.0 mm and the segment thickness is 40 mm<sup>4</sup>. All of the 123 different mirror surfaces match a single best-fit sphere within about 180 um Peak-to-Valley (P-V) (the maximum amount of warping required).

SMP was developed and used effectively by Nelson et. al.<sup>1,2</sup> for the fabrication of 84 Keck telescope primary mirror segments (including spares). Experience and literature from processing the Keck segments is used here as a baseline.

After SMP on slightly oversize blanks the segments are edged to their final shape and the mirror surface is then finished with Ion Beam Figuring (IBF). The required SMP accuracy is therefore determined by the capture range of IBF (about 2 um P-V), less any allowance for springing from edging. This allows SMP to neglect some of the higher order surface terms and leads to some simplifications. In practice IBF removal rates are much slower than SMP so for minimum cost the actual SMP-to-IBF handoff point will occur at the limit of SMP.

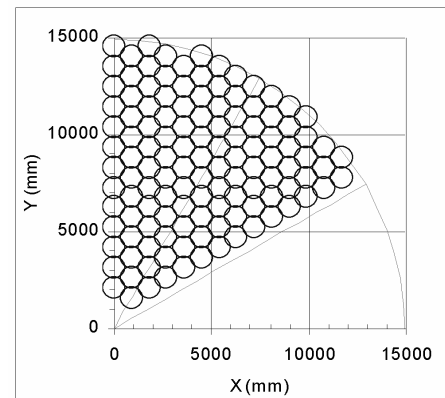


Figure 1. TMT segment layout

### 3. DEFLECTION AND STRESS ANALYSIS

#### 3.1. Warping Theory

The description of the surface in local segment coordinates is given by Nelson and Temple-Raston<sup>5</sup>.

The segment coordinate system, shown in Figure 2, is centered on the part with the z-axis normal to the mirror surface. In this orientation each term of the segment shape can be represented by a single value, or polar monomial coefficient ( $\alpha_{mn}^{SEG}$ ), because the orthogonal terms vanish. The segment surface is described in the segment coordinate system by:

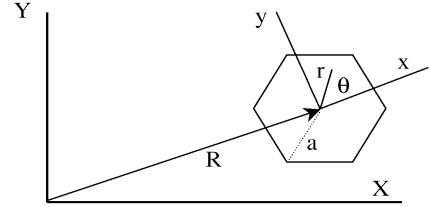


Figure 2.  
segment coordinate system

$$z(\rho, \theta) = \sum_{mn} \alpha_{mn}^{SEG} \rho^m \cos(n\theta) \quad \text{for even } m-n, \text{ and } m \geq n \geq 0, \quad (1)$$

where the normalized radius  $\rho = r/a$  in Figure 2. Explicit equations for calculating each  $\alpha_{mn}^{SEG}$  through 4th order are<sup>5</sup>:

power	$\alpha_{20}^{SEG} = \frac{a^2}{k} \left[ \frac{2 - Ke^2}{4(1 - Ke^2)^{3/2}} \right]$	
astigmatism	$\alpha_{22}^{SEG} = \frac{a^2}{k} \left[ \frac{Ke^2}{4(1 - Ke^2)^{3/2}} \right]$	
coma	$\alpha_{31}^{SEG} = \frac{a^3}{k^2} \left[ \frac{Ke[1 - (K+1)e^2]^{1/2}(4 - Ke^2)}{8(1 - Ke^2)^3} \right]$	(2)
trefoil	$\alpha_{33}^{SEG} = \frac{a^3}{k^2} \left[ \frac{K^2 e^3 [1 - (K+1)e^2]^{1/2}}{8(1 - Ke^2)^3} \right]$	
spherical aberration	$\alpha_{40}^{SEG} = \frac{a^4}{k^3} \left[ \frac{8(1+K) - 24Ke^2 + 3K^2 e^4(1-3K) - K^3 e^6(2-K)}{64(1 - Ke^2)^{9/2}} \right]$	
secondary astig.	$\alpha_{42}^{SEG} = \frac{a^4}{k^3} \left[ \frac{Ke^2[2(1+3K) - (9+7K)Ke^2 + (2+K)K^2 e^4]}{16(1 - Ke^2)^{9/2}} \right]$	
quadrafoil	$\alpha_{44}^{SEG} = \frac{a^4}{k^3} \left[ \frac{K^2 e^4 [1 + 5K - Ke^2(6+5K)]}{64(1 - Ke^2)^{9/2}} \right]$	

where  $k$  = the parent mirror paraxial ROC (60000 mm),  $K$  = the conic constant (-.999114),  $R$  = the off-axis distance of the segment center,  $e=R/k$ , and  $a$  = the segment radius.

The amount of warping required is the difference between the sphere polished into the surface and the desired aspheric surface shape. If  $k_B$  is the ROC of the blank in its stress-free state, then the stressing coefficients are:

power	$\alpha_{20}^{STR} = a^2 / (2k_B) - \alpha_{20}^{SEG}$	
astigmatism	$\alpha_{22}^{STR} = -\alpha_{22}^{SEG}$	
coma	$\alpha_{31}^{STR} = -\alpha_{31}^{SEG}$	
trefoil	$\alpha_{33}^{STR} = -\alpha_{33}^{SEG}$	(3)
spherical aberration	$\alpha_{40}^{STR} = a^4 / (8k_B^3) - \alpha_{40}^{SEG}$	
secondary astig.	$\alpha_{42}^{STR} = -\alpha_{42}^{SEG}$	
quadrafoil	$\alpha_{44}^{STR} = -\alpha_{44}^{SEG}$	

Table 1 shows the resultant stressing coefficients and P-V stressing departures for the extreme (innermost and outermost) TMT segments, using the minimum stress blank ROC established later in this report. P-V values that are small relative to the IBF capture range may be neglected for SMP.

Table 1. TMT stressing coefficients - ( $k_B = 62454 \text{ mm}$ )

description	m n	innermost segment		outermost segment	
		$\alpha_{mn}^{STR}$ mm	P-V <sub>mn</sub> um	$\alpha_{mn}^{STR}$ mm	P-V <sub>mn</sub> um
power	2 0	-0.1152	115.2	0.0514	51.4
astigmatism	2 2	0.00135	2.7	0.0828	165.6
coma	3 1	0.00090	1.8	0.00627	12.5
trefoil	3 3	0.00000	0.00	-0.00009	0.19
spherical aberr.	4 0	0.00007	0.07	0.00006	0.06
secondary astig.	4 2	0.00000	0.00	-0.00001	0.01
quadrafoil	4 4	0.00000	0.00	0.00000	0.00

It turns out that, for an extremely wide range of optical surfaces including TMT, the desired surface shapes can be achieved by the application of appropriate, continuously varying, tangential moments and shear (normal) forces only around the perimeter of the part. No warping loads are required in the interior of the part.

Nelson et. al.<sup>1,2</sup> give the method for calculating the continuous moment and shear force densities required around a circular segment perimeter to achieve the desired warping. Expressions for these, along with the relationships between the polar monomial coefficients, Zernike coefficients, and P-V amplitudes for the various terms are summarized in Table 2.

Table 2. Polar monomial coefficient relationships

description	order	azimuthal periodicity	polar monomial coefficient	$\alpha_{mn}$ / Zernike coefficient	P-V amplitude / $\alpha_{mn}$	continuous	continuous	uniform
						moment density	shear force density	reaction pressure
	m	n	$\alpha_{mn}$	$\alpha_{mn}/C_{mn}$	P-V <sub>mn</sub> / $\alpha_{mn}$	$M_{mn}$ N-m/m	$V_{mn}$ N/m	$q_{mn}$ MPa
power	2	0	$\alpha_{20}$	2	1	$(2D/a^2)(1+v)\alpha_{20}^{STR}$	0	0
astigmatism	2	2	$\alpha_{22}$	1	2	$(2D/a^2)(1-v)\alpha_{22}^{STR}$	$2M_{22}/a$	0
coma	3	1	$\alpha_{31}$	3	2	$(2D/a^2)(3+v)\alpha_{31}^{STR}$	$-M_{31}/a$	0
trefoil	3	3	$\alpha_{33}$	1	2	$(6D/a^2)(1-v)\alpha_{33}^{STR}$	$3M_{33}/a$	0
spherical aberr.	4	0	$\alpha_{40}$	6	1	$(4D/a^2)(3+v)\alpha_{40}^{STR}$	$-8M_{40}/a(3+v)$	$(64D/a^4)\alpha_{40}^{STR}$
secondary astig.	4	2	$\alpha_{42}$	4	2	$(12D/a^2)\alpha_{42}^{STR}$	$-(1+v)M_{42}/a$	0
quadrafoil	4	4	$\alpha_{44}$	1	2	$(12D/a^2)(1-v)\alpha_{44}^{STR}$	$4M_{44}/a$	0
						$D = Et^3 / 12(1-v^2)$		

where E = modulus of elasticity, v = Poisson's ratio, and t = thickness of the segment.

For N equally spaced levers at  $\theta_L$  (L=1 to N), the discrete moment and shear force required at each lever is:

$$M_L(\theta_L) = \frac{2\pi a}{N} \sum_{mn} M_{mn} \cos(n\theta_L) \quad \text{for even m-n, and, } m \geq n \geq 0 \quad (4)$$

$$V_L(\theta_L) = \frac{2\pi a}{N} \sum_{mn} V_{mn} \cos(n\theta_L) \quad \text{for even m-n, and, } m \geq n \geq 0 \quad (5)$$

where  $M_{mn}$  and  $V_{mn}$  are the continuous moment and shear force densities respectively from Table 2.

Generally for SMP on TMT only the first three terms in Table 2 will be significant. The trefoil term gets borderline towards the outer segments but its magnitude (about 0.2 um P-V), and the magnitudes of the moments and shears required to affect it, are near the resolution limits of the force actuators and feedback sensors. The higher order terms are included in Table 2 to show the moments and forces that would be needed to *remove* any of these higher order terms if they would be inadvertently introduced to the part during the polishing process.

### 3.2. Explicit Stress Calculation

Assuming classical (thin) plate theory, the bending stress at any point on the surface of a segment is directly proportional to the local bending curvatures there. The local curvatures for each term are equal to the second derivatives of that term's Zernike equation in Cartesian form. The relationship between Zernike and polar monomial coefficients is shown in Table 2.

The failure criterion for brittle materials in tension is the maximum principle stress. It turns out conveniently that the maximum principal stresses occur on the local x-axis at the edge of the part, at locations where the in-plane shear stresses are zero.

Combining the above, the maximum bending stress in the part is:

$$\sigma_{\text{MAX}} = \frac{Et}{a^2} \left[ \frac{1}{(1-\nu)} \alpha_{20}^{\text{STR}} + \frac{1}{(1+\nu)} \alpha_{22}^{\text{STR}} + \frac{(3+\nu)}{(1-\nu^2)} \alpha_{31}^{\text{STR}} + \frac{3}{(1+\nu)} \alpha_{33}^{\text{STR}} + \frac{(5+\nu)}{(1-\nu^2)} \alpha_{40}^{\text{STR}} + \dots \right] \quad (6)$$

(power)                      (astigmatism)                      (coma)                      (trefoil)                      (sph. aberr.)

For the two dominating 2nd order terms (power and astigmatism) the bending stress is actually constant over the entire segment surface and independent of the size of the blank.

The maximum stress for the two 3rd order terms varies linearly with the size of the blank. However the maximum coma stress is not more than about 15% of the total stress to begin with so making the blanks 5 or 10% oversize increases the maximum stress levels only slightly. Trefoil and the 4th and higher order stress terms are negligible. Only the first three stress terms are significant for TMT.

### 3.3. Validation of Predicted Deflections and Stresses

We performed Finite Element Analyses (FEA) on a constant thickness segment, using the discrete loads generated by equations (4) and (5), for the innermost and outermost segments, on both a term-by-term basis and all together. We found the deflection and stress results to match the theoretical predictions (equations (1) and (2)) within 2 to 3 %, validating the theory and the FEA models against each other.

The applied loads were then adjusted slightly to achieve the best possible match with the desired surface shapes. We found that the lower order terms (power) match the theory better and the higher order terms (coma) match the theory worse. This is offset to considerable extent by the fact that the higher order terms are smaller.

For constant thickness segments with FEA we were able to get the shapes theoretically correct, for all terms combined, within about 0.5 um P-V all the way to the edges, and within about 0.2 um P-V if we ignore (cut away) 60 mm from the edges. There is an edge effect under the bond pads which adds on the order of 2-3X to the P-V errors at the edges.

It should be noted that the FEA results are based on somewhat idealized models and probably show the best that should be expected. Also note that warping form error is only one component in the total SMP error budget.

## 4. DESIGN TRADE STUDY

### 4.1. COC Versus CP Trade

The Keck segments were processed on Center Over Center (COC) equipment. It has been proposed to examine Continuous Polishing (CP) and Center Over Center (COC) configurations (among others) for the most cost effective production.

CP (also called Planetary Polishing) uses a large annular pad rotating face up on a vertical axis, with parts placed face down on the pad and guided by a septum. The outside diameter of the pad is typically at least three times the diameter of the part, which leads to a very large (and expensive) machine. The main advantage of CP is that there is room to run up to three parts simultaneously on one machine. CP machines are typically configured for flat surfaces, and the 60 meter TMT ROC would have only 42 mm of sag across a 4.5 meter diameter pad.

COC (also called over-arm) polishing uses a fixed vertical spindle on the bottom and a laterally oscillating vertical spindle with a ball or universal joint on top. In this case the part would be mounted on the lower spindle face up and the tools would be driven on the upper spindle (see Figure 4). Both the upper and lower spindle speeds are adjustable and the applied tool pressure is easily varied.

We have characterized existing grinding and polishing processes and scaled them up to TMT for comparison. These include COC High Speed Grinding, COC High Speed Pad Polishing, COC High Speed Pitch Polishing, COC Figuring Pitch Polishing, CP Pad Polishing, CP High Speed Pitch Polishing, and CP Figuring Pitch Polishing. In general COC material removal rates are about 5 times greater than with CP, mostly due to the higher surface speeds obtainable with COC. COC machines can be run slowly for figuring but CP machines cannot be run fast for high removal rates.

We estimate for an entirely COC process that about eight COC machines would be required. A CP process would require at least two CP machines, without eliminating the need for two or three COC machines for grinding and polish out.

A major advantage of multiple COC machines is the ease of reconfiguring them to optimize throughput. For example, imagine 8 essentially identical COC machines configured with tools as follows: 1 back side grind, 1 back side pad polish, 1 front side grind, 1 front side pad polish, 2 front side pitch polish, and 2 front side figure polish. If this allocation of machines is not optimum it is easy to shift machine time, or even entire machines, from the steps that turn out to be faster to the steps that turn out to be bottle necks, thereby balancing the process flow. This is nearly impossible to do on a small number of CP machines running multiple parts per machine.

There are fairly large potential time savings around surface measurement if the measurements can be made quickly. This also favors COC with the parts face up. The parts can be measured in situ with a portable LVDT array. Handling the parts for measurement would be much more cumbersome with CP.

Also with the warping fixture on the bottom in COC its weight does not need to be managed as it does with it above the part in CP.

Due to the wider variety of capital equipment and tools that would have to be developed for CP, we estimate for the same throughput a cost differential of about \$1.5 million in favor of COC. For the above reasons we recommend an entirely COC process with about eight COC machines.

#### 4.2. Segment Material Options and Properties

The material will be low thermal expansion glass or glass-ceramic (Zerodur, ULE, Astrosital, etc.)<sup>6</sup>. Keck used Zerodur (Schott). All analyses and results presented here assume Zerodur.

Schott technical bulletin TIE-33<sup>7</sup> has extensive information on the strength of Zerodur with various surface finishes. Examination of the data yields the interesting result that even though the characteristic strengths (of test samples) with polished and etched surfaces are several times greater than for ground surfaces, the larger Weibull spread in polished and etched surface data yields design strengths that are actually lower for polished and etched surfaces than for ground surfaces of this large size and low probability of failure requirements, as shown in Table 3. This was confirmed by Schott<sup>8</sup>.

Table 3. Zerodur Design Strengths (MPa / psi)

	for admissible probability of failure:	
	1/10,000	1/1,000
from Schott TIE-33 <sup>7</sup> , 1.3 m blank, stressed over entire surface		
Optical polish	4.9 / 710	7.6 / 1110
64 grit ground then etched	5.5 / 800	8.2 / 1190
320 grit loose SiC ground	9.2 / 1340	11.2 / 1620
from John Pepi <sup>9</sup> , Keck experience		
Keck value for global warping stresses	2.1 / 300	
including stress concentrations (also = NASA std.)	4.8 / 700	

Based on the above we assume a global bending design strength of 2.1 MPa (300 psi) and a safe limit including stress concentrations of 4.8 MPa (700 psi).

If Zerodur is used its delayed elastic effect needs to be taken into account during surface measurements. When the loads are released the immediate spring back is not 100%. Roughly the last 1% of elastic strain is released over a period of hours and days following removal of the warping loads. This effect is completely reversible and predictable but must be accounted for during measurements of the accuracy required here. This delayed elastic effect is described in detail by Pepi<sup>10</sup>.

With ULE, increasing the thickness about 10% would yield similar gravity weight deflections and warping loads, with stresses about 20% less than with Zerodur. The relative cost of ULE blanks is TBD.

### 4.3. Mirror Blank Geometry

#### 4.3.1. Material Cost

The smallest flat (ungenerated) blank that could conceivably be used would be a hex about 1.22 m across and 43 mm thick, requiring a total mass, assuming Zerodur, of about 200,000 lb (about 2.5 times the mass required for the two Keck primary mirrors). 2005 pricing for Zerodur is about \$75/lb retail. If we use an estimate of \$60/lb for high volume production pricing of Zerodur then 861 blanks of this minimum size and shape would cost about \$12 million. Clearly even a few percent change in material volume would have a significant impact on program cost. In practice larger blanks than this minimum will be required.

For an order this size custom molds would be made and the parts would be cast near net shape to minimize material waste. This gives the potential of using hexagonal blanks, which in principle uses up to 17% less material than round blanks of the same outside dimension.

Table 4 shows comparative blank material program costs for the above assumptions.

1.30 m round blanks - baseline, least risk, most expensive -	\$16.4M
1.22 m round blanks - smaller, more risk, less material cost -	\$14.6M
1.30 m hex blanks - more development time and risk, less material cost -	\$13.6M

Significant potential cost savings with hex blanks are apparent. Several factors take away from this potential savings however.

The first is that a hexagonal shape is probably a bit (although probably not terribly significantly) more expensive to edge than a round. Other factors taking away from potential cost savings with hex blanks are described in the following section.

#### 4.3.2. Tooling, development, and processing complexity

SMP of round blanks was accomplished on the Keck mirrors and the method is covered quite thoroughly in the literature<sup>1,2</sup>.

Tooling for round blanks would be totally rotationally symmetric, with the advantage of minimizing the number of unique parts while maximizing the number of common parts, which helps reduce cost.

Although Lubliner<sup>11</sup> lays out a theoretical basis for warping hexagonal blanks, to our knowledge SMP on hex blanks has not been demonstrated. Significant development work, time, and risk would be added to the program over round blanks. Processing difficulty may also be increased with hex blanks as there is "a built-in theoretical imprecision" which cannot be backed out analytically, so figuring must proceed on a strictly iterative basis in the optical shop<sup>11</sup>.

None of these issues seem insurmountable but would definitely involve additional time, expense, and risk over that needed for round blanks, taking away from material cost savings obtained using hexagonal blanks.

#### 4.3.3. Blank Size

In practice, whether hex or round, there are a few effects that require the blanks to be processed through SMP at least slightly larger than the finished segment size. If any of these effects are too large to be fixed by IBF they must be kept outside the final hex profile and cut away. Edge effects are typically maximum at the edge and decreasing exponentially going inward. Obviously the magnitude and decay rate of these effects dictates the amount of segment edge margin required.

First, the edges will roll a bit from polishing. The magnitude and extent is difficult to predict but we estimate an edge margin of 10-20 mm would probably be sufficient here.

Second, there may be significant edge bending and/or scalloping effects from the warping fixture and loads themselves. An edge bending effect is caused by an imperfect radial boundary condition where the warping loads are applied. For example, with pads bonded to the bottom perimeter of the segment (not on the cylindrical surface on the neutral axis as in Keck) a small amount of un-loaded material exists between the pad and the edge. These effects may extend inward a distance on the order of at least the thickness of the part. FEA estimates of the magnitude of this edge effect are up to about 0.3 um with meniscus blanks.

Scalloping is a periodic circumferential effect caused by the discrete bond pads and stepwise varying applied loads. FEA predicts a scalloping magnitude on the order of 0.1 um at the edge, decreasing to maybe 0.02 um at 50 mm in from the edge. The slopes at these scalloping and edge effects are well within the capability of IBF.

The largest of all these effects determines the amount of edge margin needed on the blanks.

#### 4.3.4. Springing When Edging To Size

We used an FEA method suggested by John Pepi<sup>9</sup> to estimate the springing of a segment when hexed to final size after SMP and before IBF. This method simulates releasing 20 psi of uniform isotropic residual compressive stress in the material that is cut away. (Residual stress values of 10-50 psi were measured previously for Zerodur<sup>12</sup> and 20 psi was recommended by Pepi.) FEA cases were run, removing varying amounts of edge margin, for both round and hex blanks. The result is a change in curvature accompanied by a small edge effect.

If the FEA assumptions described above are valid the amount of springing will be well within tolerable limits. The resultant FEA springing predictions are on the order of 0.05 um P-V across the entire part, with a .01-.02 um P-V edge effect, and are significantly less than the springing suggested with Keck<sup>13</sup>: "...For Keck...cutting resulted in surface deformations of order 1 micron." There are several possible explanations for this discrepancy:

- differences between TMT and Keck segment geometry
- variations in the magnitudes and distributions of actual residual stresses in the real parts (i.e. stresses not uniform and isotropic),
- overly idealized FEA models

We applied the same FEA method to the Keck segment geometry and the result was that the Keck springing was about double the present TMT case. This suggests that, since the Keck springing was manageable, as long as TMT uses material with similarly low internal stress, the TMT springing should be manageable as well.

FEA results show P-V change roughly proportional to the *volume* of material removed, and, as might be expected, slightly more springing with round blanks than with hex blanks of the same outside dimension.

One advantage of round blanks is that most of the lever bond areas and edge effects are further away from the final part profile. Only the areas near the six corners have substantial risk of edge effects straying within the finished clear aperture. With hex segments all the arms are bonded, and edge effects occur, close to the final clear aperture.

In summary, the amount of springing when edging to size does not appear to be a problem, and does not appear to be great enough to significantly favor hex over round blanks on that basis.

#### 4.3.5. Meniscus versus Flat Back Blanks

It has been suggested that flat back blanks might be less expensive and/or easier to process. However the moments and shears required to achieve the desired shapes with SMP assume constant plate thickness (i.e. meniscus mirror blanks). Therefore flat back parts with variable thickness will depart from plate theory. Here we attempt to quantify how much for TMT.

We performed FEA on flat back segments using the same procedure described previously for validating the FEA models with meniscus blanks. We kept the edge thickness at 40 mm and made the back surface flat, giving a center thickness of about 37.1 mm.

After tuning the applied loads we were able to get the correct shapes within about 1.5 um P-V all the way to the edge, and within about 0.6 um P-V by cutting away 60 mm from the edges -- about 3 times worse than with meniscus blanks. With a total SMP error budget of 2 um these numbers are large enough to cause concern. Some additional type of compensation would have to be developed to reduce these values. Again maybe not an insurmountable problem but would require additional effort.

We also didn't discover any real technical advantage with flat back blanks. Preference for flat back parts seemed to come from the shop floor where that is simply "what they are used to".

We don't see any increased difficulties with meniscus blanks over flat back blanks, and the warping theory is much cleaner with meniscus blanks.

#### 4.3.6. Optimum Blank ROC

Results from stress analysis show that a single blank ROC may be used for all the segments. This also means a single ROC for the grinding, polishing, and measuring tools. The following sections evaluate different criteria for determining the optimum blank ROC.

#### 4.3.6.1. Minimum Stress

It is straightforward to find the blank ROC that minimizes the global maximum warping stress in all the segments. Using this blank ROC the maximum bending stresses in the innermost and outermost segments are equal. This ROC as determined explicitly by spreadsheet is 62467 mm, and yields a maximum bending stress in the innermost and outermost segments of about 1.6 MPa (230 psi), as shown in Figure 3 for all 123 segments as a function of location on the parent. These stress values at the innermost and outermost segments were verified with FEA, and are about 3/4 of the design limit for Zerodur.

A reasonable tolerance on the delivered blank ROC is +/- 80 mm which would yield a stress variation of about +/- 3 %.

The minimum stress blank ROC is empirically very close to the power term of a segment located at a radius on the

parent =  $\sqrt{2/3}R_{\max}$ , or

$$k^* = \frac{\left[1 - \frac{2}{3}K\left(\frac{R_{\max}}{k}\right)^2\right]^{\frac{3}{2}}}{\left[1 - \frac{1}{3}K\left(\frac{R_{\max}}{k}\right)^2\right]} k \quad (7)$$

where  $R_{\max}$  = the parent maximum radius (15000 mm), and  $k^*$  = the segment ROC at  $R = \sqrt{2/3}R_{\max}$  (62485 mm).

#### 4.3.6.2. Minimum Material Removal

In the interest of maximum processing speed we found that a ROC of about 61000 mm would give the least material removal overall. This ROC is much closer to the paraxial ROC and would require stress levels of about 2.37 MPa (343 psi) at the outermost segments - about 50% greater than with the minimum stress ROC described in the previous section. The maximum stress in the innermost segment would be only 0.78 MPa (114 psi), a difference of a factor of 3 in maximum stress between the innermost and outermost segments.

Further, minimum material removal only saves about 1/2 to 2 hours per part in the first grinding step. The aspheric volume removed is only about 1/4 of the volume removed for stress relief at this step. Assuming an average savings of 1 hour per part and a shop rate of \$100/hr this would amount to a savings of only about \$86,000 over the life of the program, not significant enough in our judgment to justify the much higher stresses and load levels.

#### 4.3.6.3. Mean ROC

This is the ROC suggested in Reference 6 and is equivalent to the power term in a segment 71% of the way out on the parent, with half the segments inside and half the segments outside that location. Using this blank ROC (61847 mm) the maximum stress in the outer segment would be 1.96 MPa (284 psi), about 25% higher than the value using the minimum stress ROC described above, while the maximum stress at the innermost segment would be only 1.19 MPa (173 psi), a difference of a factor of 1.64 in maximum stress between the innermost and outermost segments.

#### 4.3.6.4. Conclusions re: Optimum Blank ROC

We recommend using a blank ROC that minimizes the global maximum bending stress in the segments. In addition to minimizing risk of catastrophic failure of a segment during SMP, there are cascading benefits. The lower corresponding maximum loads reduce the demands on the warping fixture design and components. And the more even distribution of loads across the segments requires less dynamic range from the actuators and force sensors.

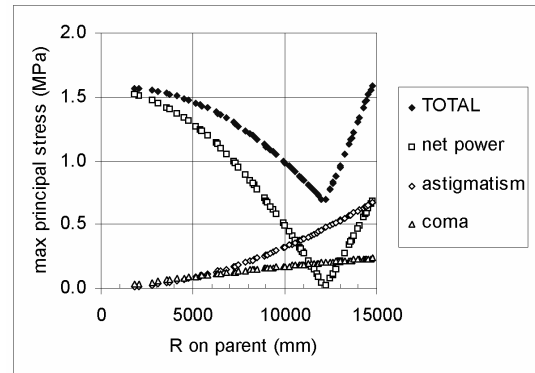


Figure 3. Maximum segment bending stress for blank ROC = 62467 mm

## 5. WARPING FIXTURE CONCEPTUAL DESIGN

### 5.1. Spherical Processing

One way to look at the problem is basically as a spherical processing task with warping superimposed. A Center Over Center spherical grinding and polishing set-up is illustrated in Figure 4.

Using a 14 inch test plate, surface irregularity can be monitored relatively easily to within about 2  $\mu\text{m}$  over the entire surface, and with care to about 1  $\mu\text{m}$  over the entire surface. Radius measurements can be made using a large spherometer. Conventionally the ROC would be controlled by varying the COC machine parameters (stroke and offset). However here there is also the possibility of using the warping fixture itself to control the ROC.

### 5.2. Gravity Supports and Gravity Deflection

The segment must be supported in a manner that allows it to accurately flex to the desired shapes, both during grinding and polishing and relaxed (unloaded) for measurements.

There must be sufficient number of support points to prevent excessive deflections between the pads, both during measurement and during grinding and polishing. Since the support structure floats the support pads must also be carefully located to evenly distribute and balance the support loads. Imbalanced support loads would introduce undesirable static deflections of the part.

A whiffle tree or hydraulic pads are two options for accomplishing this. Figures 5 and 6 illustrate these concepts.

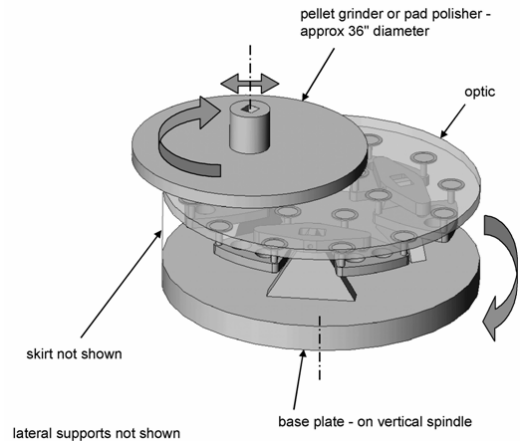


Figure 4. Center Over Center Grinding and Polishing Set-up

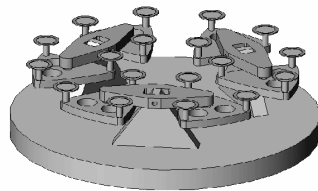


Figure 5. 18 pad whiffle tree

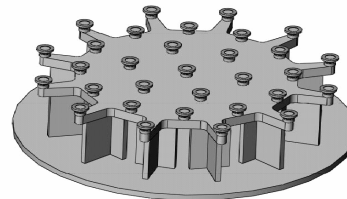


Figure 6. 31 hydraulic pads

Both supports illustrated would have gravity deflections on the order of 0.06  $\mu\text{m}$  P-V, the larger pads on the whiffle tree making up for the smaller number of pads.

The part and warping fixture will be rotating on the lower spindle during grinding and polishing and increased rotation speeds are desirable, therefore centrifugal force effects will need to be considered. Designs that are less sensitive to centrifugal force will be favored.

A hydraulic pad design was used on Keck. Without a strong reason to change it we recommend a similar approach. Each hydraulic pad can have its own valve to essentially lock it in place for polishing after the warping loads are applied and the part is allowed to float to shape.

### 5.3. Lateral Supports and Clocking Control

The segment must be supported against lateral (side) loads that would tend to shear the part radially off the fixture and against clocking (rotation) on the fixture. Figure 7 shows two examples of six reaction arms attached to the warping fixture levers and reacting through the bond pads away from the hex aperture. There are many options here. While, theoretically, exactly three arms are required to constrain the part and more than three over-constrain it, the lateral loads on the Keck warping fixture were reacted through all 24 lever arms without problems. With care the arms can be assembled without introducing excessive stray loads. The arms can be athermalized (designed to be insensitive

to temperature changes) if necessary. A greater number of reaction paths distributes the reaction loads more evenly around the part and help minimize local stray bending effects. Up to 12 reaction arms would be easy to implement and would give the flexibility to remove some arms if advantageous.

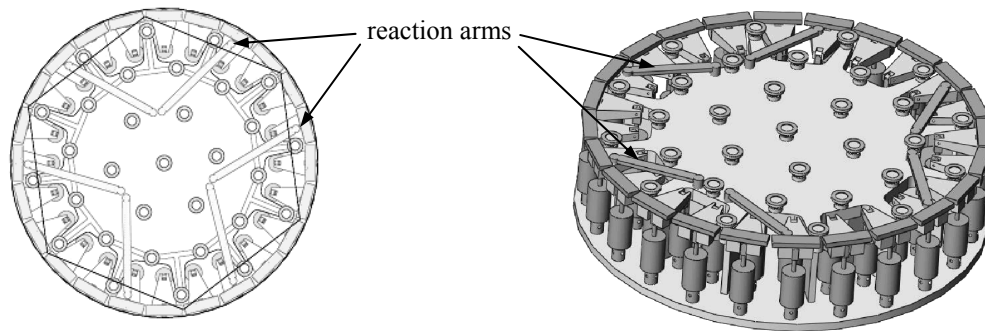


Figure 7. Lateral Supports and Clocking Control Examples

#### 5.4. Contamination Control

The high speed COC process will generate a spray of grinding and polishing slurry that must be kept out of the warping mechanism and any other delicate or electronic components on the warping fixture. Ideally, we envision a rectangular plastic film wrapped around and taped to the outside perimeter of the part and to the base plate of the warping fixture. This would mean that the base plate would have the same profile as the blank. The most obvious impacts of this are that the bond pads are attached to the bottom surface of the segment near the edge, not on the outside cylindrical surface as in Keck, and that the warping mechanism is wrapped underneath the blank and entirely inside the part perimeter.

#### 5.5. Levers, Bond Pads and Warping Loads

Keck SMP used 24 levers. Without a compelling reason to change it, we used the same number of levers for our baseline design. If trouble is encountered with cost or space constraints, it may be possible to reduce the number of levers, perhaps to 18.

The bond pads are epoxied to the outer perimeter of the segment back surface using a separate alignment fixture. The bonds must be stress-free so that mirror shape doesn't change when the pads are removed. After SMP the pads are removed by softening the epoxy with heat.

For Zerodur segments 40 mm thick and using 24 levers the approximate ranges of required edge loads are:

- edge moment: +/- 68 N-m (600 in-lb)
- edge shear: +/- 110 N (25 lb)

FEA predicts stress concentrations (near and under bond pads with radiused corners) of approximately 2.0-2.4, i.e. stresses about 3.2-3.8 MPa (460-550 psi) which are again about 3/4 of the design limit for Zerodur.

#### 5.6. Force Actuators

With 24 arms there are 48 force actuators, two on each lever arm. A suggested warping actuator design is shown in Figures 8 and 9.

The lever geometry shown in Figure 9 would require an actuator force range of about +/- 700 N (158 lb).

The force actuators must be very accurate and reliable in a set-and-hold application. There are at least a couple options:

1) a motor driven screw compressing and extending a spring, with a load cell in series to sense the applied force. A die spring with a rate of about 250 lb/in (1 inch diameter, 3 to 3.5 inch free length) would be about right.

2) a double acting pneumatically actuated diaphragm cylinder. This has the advantage that the pressure sensors can be located remotely, and very accurate pressure sensors are available. However the consequences of any leak in the pneumatic system may be too much to bear and continuous real-time control of 48 pressures seems fraught with difficulties.

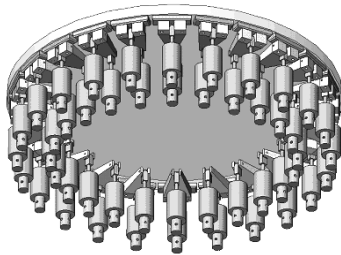


Figure 8. Warping Mechanism - (gravity and lateral supports removed for clarity)

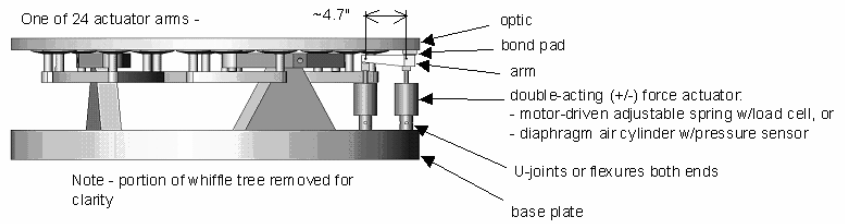


Figure 9. Actuator Detail

### 5.7. Errors in Warping and Tolerances On Applied Loads

The final accuracy of SMP may ultimately be limited by the accuracy of the applied load sensors. Whatever type of actuator is used, extremely accurate and stable means of measuring the applied loads will be required. We estimate that a load sensing error of 0.1% of full scale with the current actuator and lever geometry will yield a surface error of about 0.5  $\mu\text{m}$  P-V at the edge of the segment.

Load sensors can be individually calibrated over force, temperature, and humidity ranges, but also need to be extremely stable over time. Temporal stability of the load sensors may be their most demanding requirement.

### 5.8. Warping Mechanism Control Diagram

Figure 10 shows a control diagram for motor driven spring actuators with load cells. Control of a pneumatic actuator with pressure sensors would be similar.

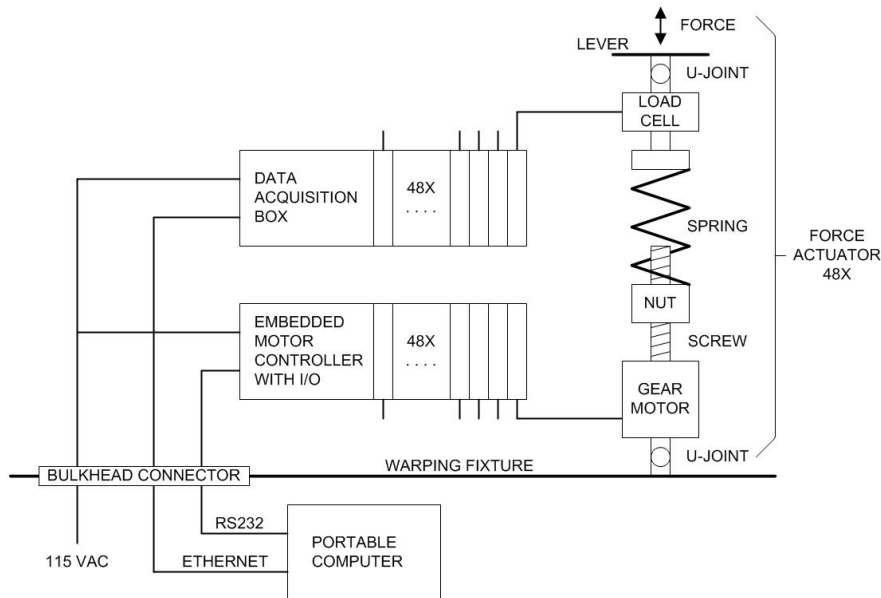


Figure 10. Warping Mechanism Control Diagram

## 6. ERROR BUDGET

A preliminary SMP error budget is presented in Figure 11 below for purposes of review and future refinement. Values are estimates and are RSSd for a total error of 2.0 um P-V prior to IBF.

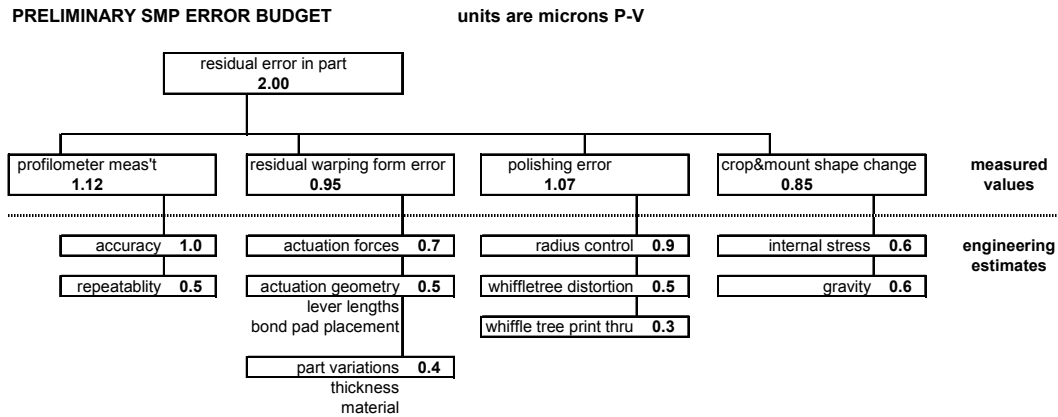


Figure 11. Preliminary Error Budget

## 7. CONCLUSIONS

Stressed Mirror Polishing of 861 TMT segments under the constraints provided looks feasible.

If the blank radius of curvature is chosen to minimize the global maximum warping stress then induced stresses for the present segment definition appear to be about 3/4 of allowable values.

In our estimation most if not all of the material cost savings with smaller and/or hex blanks will be offset by the increased development time, complexity, risk, etc. More accurate knowledge of expected material price is needed to assess this trade.

If desired, select blank shape (hex or round) by trading material cost savings against increased development time, expense, and risk.

If desired, select blank size by trading material cost savings against required edge margin.

## 8. RECOMMENDATIONS

In the interest of expediency we recommend a baseline conservative approach that follows the Keck process where practical with improvements to throughput, unless material cost pressures require more aggressive development (hex blanks, reduced edge margins). I.e.:

- 1.3 m round constant-thickness blanks,
- processed COC face up,
- warped by moments and shears at the perimeter,
- blank ROC chosen to minimize bending stresses,
- each segment married to one of 8 to 10 robotically controlled warping fixtures, the pair traveling together though a multi-station process,
- higher tool speeds and pressures,
- and rapid surface measurement capability.

Depending on the anticipated cost of the mirror blank material, consider:

- whether potential material cost savings with hex blanks justifies further investigation (refinement of hexagonal warping theory and evaluation of additional tooling complexity and cost), and
- whether potential material cost savings with smaller blanks justifies further investigation (more refined examination of scalloping and edge rolling).

Considering that the predicted warping stresses are about 3/4 of allowable values, determine if there is any reason outside the scope of this paper (e.g. in-use gravity deflections) to change the segment parameters (e.g. increase thickness).

Finally, Tinsley strongly recommends that the TMT program fund the design, construction and verification of a full scale warping fixture. This fixture can be used on a large existing Tinsley COC machine to study and determine SMP process parameters, convergence rates, and speed and accuracy limits of SMP on TMT sized segments. Since material removal rates with IBF are much slower than with SMP, mirror segment cost will be minimized by fully optimizing the SMP process and driving the surface error at SMP-to-IBF handoff to an absolute minimum. Building a full scale SMP fixture will yield valuable insight on the SMP process limits, and more accurate cost and schedule estimates for production of TMT primary mirror segments.

## ACKNOWLEDGEMENTS

We would like to thank Jerry Nelson and John Pepi for freely sharing the results of their prior work and experiences processing the Keck segments.

The authors gratefully acknowledge the support of the TMT partner institutions. They are the Association of Canadian Universities for Research in Astronomy (ACURA), the Association of Universities for Research in Astronomy (AURA), the California Institute of Technology and the University of California. This work was supported, as well, by the Canada Foundation for Innovation, the Gordon and Betty Moore Foundation, the National Optical Astronomy Observatory, which is operated by AURA under cooperative agreement with the National Science Foundation, the Ontario Ministry of Research and Innovation, and the National Research Council of Canada.

## REFERENCES

1. Lubliner and Nelson, "Stressed Mirror Polishing. 1: A technique for producing non-axisymmetric mirrors", TMT Report No. 61. [Applied Optics, Vol. 19, No. 14, 15 July 1980]. (Keck Observatory Report No. 21)
2. Nelson, Gabor, Hunt, Lubliner, Mast, "Stressed Mirror Polishing. 2: Fabrication of an off-axis section of a paraboloid", TMT Report No. 62. [Applied Optics, Vol. 19, No. 14, 15 July 1980]. (Keck Observatory Report No. 22)
3. Mast and Nelson, "TMT Primary Mirror Segment Shape", TMT Report 58, November 2004.
4. Stepp, "Specification for Finished Primary Mirror Segments", TMT.OPT.SPE.05.002.REL01, April 14, 2005.
5. Nelson and Temple-Raston, "The Off-Axis Expansion of Conic Surfaces", UC TMT (Keck) Report No. 91, November 1982
6. Stepp, "Specification for Primary Mirror Segment Blanks", TMT.OPT.SPE.05.001.REL01, April 15, 2005.
7. "Design Strength of Optical Glasses and Zerodur", Schott Technical Information Bulletin TIE-33, October 2004.
8. Dr. Peter Hartmann, Schott, private communication.
9. John Pepi, SSG Precision Optronics, Inc., private communication.
10. Pepi, "Delayed Elastic Effects In Zerodur At Room Temperature", Applied Optics, Vol. 31, No. 1, 1 January 1992.
11. Lubliner, "Stressed Mirror Polishing of Polygonal Plates", UC TMT (Keck) Report No. 87, July 1982
12. Pepi, "Test and Theoretical comparisons for bending and springing of the Keck segmented ten meter telescope", Itek Optical Systems.
13. Mast, Nelson, and Sommargren, "Primary Mirror Segment Fabrication for CELT", CELT Report No. 5, 5/8/00 - SPIE 2000